

## Toward a ferroelectric control of Rashba spin-orbit coupling: Bi on BaTiO<sub>3</sub>(001) from first principles

H. Mirhosseini,<sup>1</sup> I. V. Maznichenko,<sup>2</sup> Samir Abdelouahed,<sup>1</sup> S. Ostanin,<sup>1</sup> A. Ernst,<sup>1</sup> I. Mertig,<sup>1,2</sup> and J. Henk<sup>1,\*</sup>

<sup>1</sup>Max-Planck-Institut für Mikrostrukturphysik, Weinberg 2, D-06120 Halle (Saale), Germany

<sup>2</sup>Institut für Physik, Martin-Luther-Universität Halle-Wittenberg, D-06120 Halle (Saale), Germany

(Received 30 October 2009; published 22 February 2010)

As demonstrated conceptually by first-principles calculations, the Rashba spin splitting in the  $6p$  states of a Bi adlayer on BaTiO<sub>3</sub>(001) can be manipulated by the electric polarization in the ferroelectric substrate. Although this spin-electric effect is moderate, with a relative change in the splitting of about 5%, the absolute splitting of about  $0.24 \text{ \AA}^{-1}$  is unmatched. Further, the occupied  $6p$  surface states display an anisotropic dispersion and deviate significantly from the free-electron model of the Rashba effect. Our findings may pave a route for spin-electronic devices.

DOI: [10.1103/PhysRevB.81.073406](https://doi.org/10.1103/PhysRevB.81.073406)

PACS number(s): 73.20.At, 77.84.Ek, 77.84.Cg, 71.70.Ej

### I. INTRODUCTION

A key issue in spin electronics<sup>1</sup> is the manipulation of the electrons' spins by an electric field. This goal can be achieved for example by the magnetoelectric coupling in a multiferroic<sup>2–4</sup> or by the tunable strength of the Rashba spin-orbit coupling in a two-dimensional electron gas at a semiconductor interface.<sup>5–8</sup>

In an isotropic two-dimensional electron gas, the Rashba effect lifts Kramers' degeneracy.<sup>9</sup> As a consequence, the dispersion relations of the free electrons which are confined to the  $xy$  plane become split,

$$E_{\pm}(\mathbf{k}_{\parallel}) = \frac{\hbar^2 \mathbf{k}_{\parallel}^2}{2m^*} \pm \gamma_{\text{R}} |\mathbf{k}_{\parallel}| + E_0, \quad \mathbf{k}_{\parallel} = (k_x, k_y). \quad (1)$$

Here, the electronic states are labeled by + and –, and  $m^*$  is the effective electron mass. The Rashba parameter  $\gamma_{\text{R}}$  which quantifies the spin-orbit coupling strength comprises effectively two contributions:<sup>10</sup> The “atomic” contribution is due to the strong potential of the ions and the “confinement” contribution is due to the gradient of the confinement potential in  $z$  direction.

Surface states which are subject to the Rashba spin-orbit coupling have gained considerable attention in the last years.<sup>11,12</sup> A particularly large Rashba splitting  $k_{\text{R}} = |m^*| \gamma_{\text{R}} / \hbar^2$ , which is defined as the mutual shift of the split bands, is observed for adlayers of heavy elements with  $p$  valence shell on noble metal and semiconductor surfaces, e. g., Bi/Ag(111) (Ref. 13) and Bi/Si(111).<sup>14</sup> With regard to the abovementioned contributions, the strength of the Rashba spin-orbit coupling in an adlayer can be manipulated by alloying, for example of Pb and Bi (atomic contribution),<sup>15</sup> or by changing the charge density in the surface region by adatoms (confinement contribution; e. g., Refs. 16 and 17).

In this Brief Report, we propose a third route for manipulating the Rashba splitting of electronic states in an adsorbed layer: While keeping a Bi adlayer, we use a ferroelectric, here BaTiO<sub>3</sub>(001), in place of a metallic or semiconducting substrate. The idea is to (ferro)electrically control the Rashba splitting as follows. The reversal of the intrinsic electric polarization  $\mathbf{P}$  in the perovskite by an external electric field is equivalent to reversing the mutual displacements of Ti and O

atoms in [001] direction. Consequently, the charge density at the Bi/BaTiO<sub>3</sub> interface is changed, leading eventually to a modification of the Rashba splitting of the surface states in the Bi adlayer. This scenario of a “spin-electric coupling” is similar to the magnetoelectric coupling in a two-phase multiferroic, say in Fe/BaTiO<sub>3</sub>.<sup>18–20</sup>

Rashba/ferroelectric systems have a number of advantages. First, because the electric polarization  $\mathbf{P}$  is changed by an electric pulse (in contrast to a steady electric field),<sup>8</sup> the Rashba splitting would remain switched permanently. This feature makes such a system suitable for information storage devices.<sup>21</sup> Second, the deposition of adatoms could alter the surface electronic structure significantly<sup>22</sup> and switching of the splitting may be difficult or even impossible.<sup>23</sup> Thus, Bi/BaTiO<sub>3</sub> and similar systems lend themselves support for a new class of materials for spin electronics devices.

In this Brief Report, we demonstrate conceptually the proposed mechanism for a complete monolayer of Bi on BaTiO<sub>3</sub>(001). Using *ab initio* methods of computational material science, we focus on (i) the strength of the Rashba splitting in the  $6p$  surface states of Bi, (ii) the effect of switching the electric polarization in the ferroelectric substrate on the Rashba splitting of the Bi surface states, and (iii) their dispersion and spin polarization as compared to the free-electron model of the Rashba effect.

### II. COMPUTATIONAL ASPECTS

We follow the first-principles approach which has proved successful in earlier studies of two-phase multiferroics<sup>20</sup> and of Rashba systems.<sup>14,15,24</sup>

We consider a BaTiO<sub>3</sub>(001) substrate with TiO<sub>2</sub> termination; the deposited Bi atoms form a complete  $(1 \times 1)$  monolayer. The geometric structures have been obtained by the Vienna *ab initio* simulation package (VASP).<sup>25</sup> The adatoms have initially been placed at different positions and are subsequently relaxed to their equilibrium positions.

The structural data serve as input for the relativistic calculations which aim at the Rashba splitting and rely on our multiple-scattering theoretical codes for semi-infinite systems [Korringa-Kohn-Rostoker (KKR) and layer-KKR methods; e. g., Ref. 26]. A detailed analysis of the electronic

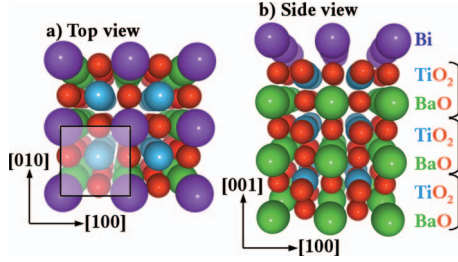


FIG. 1. (Color) Geometry of Bi/BaTiO<sub>3</sub>(001). (a) Perspective top and (b) side views of the Bi-covered BaTiO<sub>3</sub>(001) surface for electric polarization  $P_{\uparrow}$ . Spheres represent Bi (violet), Ba (green), Ti (blue), and O (red) sites. A two-dimensional unit cell is displayed in (a) as transparent square. Three BaTiO<sub>3</sub> stacks which each comprising a BaO and a TiO<sub>2</sub> layer are depicted in (b).

structure is obtained from the Bloch spectral density

$$n_{ls}(E, \mathbf{k}_{\parallel}) = -\frac{1}{\pi} \text{Im Tr } G^+(\mathbf{r}_{ls}, \mathbf{r}_{ls}; E, \mathbf{k}_{\parallel}), \quad (2)$$

which is determined from the site-diagonal Green function  $G^+(\mathbf{r}_{ls}, \mathbf{r}_{ls}; E, \mathbf{k}_{\parallel})$ . The trace involves integration over the muffin-tin sphere of site  $s$  in the two-dimensional unit cell of layer  $l$ , with  $\mathbf{r}_{ls}$  being associated with this sphere.<sup>26</sup>  $n_{ls}(E, \mathbf{k}_{\parallel})$  can be resolved further with respect to orbital composition and spin orientation.

We have checked that basic quantities are consistently reproduced by the VASP and the KKR codes. These also agree nicely with those obtained by our additional FLAPW calculations.<sup>27</sup>

### III. SURFACE GEOMETRY

In the following, we consider two major configurations which are distinguished by their intrinsic electric polarization  $\mathbf{P}$  in the bulk of the BaTiO<sub>3</sub> substrate. In accordance with the mutual displacement of the Ti and O atoms,  $\mathbf{P}$  is along the [001] direction which is taken as  $z$  direction. For  $\mathbf{P}$  pointing

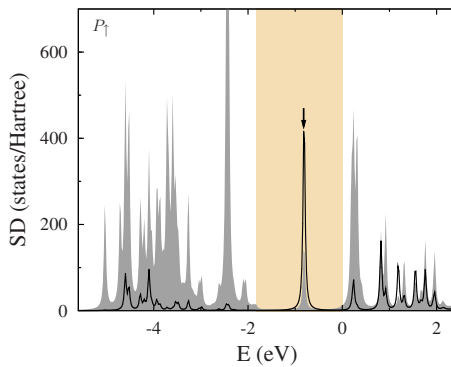


FIG. 2. (Color online) Surface electronic structure of Bi/BaTiO<sub>3</sub>(001) for  $P_{\uparrow}$ . Bloch spectral densities (“SD”)  $n(E, \mathbf{k}_{\parallel})$  are shown for the Bi adlayer (line) and for the adjacent BaTiO<sub>3</sub> stack (filled) at  $\bar{\Gamma}$  ( $\mathbf{k}_{\parallel}=0$ ). The underlying rectangle marks the fundamental band gap; the conduction band minimum is taken as energy zero. The Bi 6p surface states are indicated by an arrow.

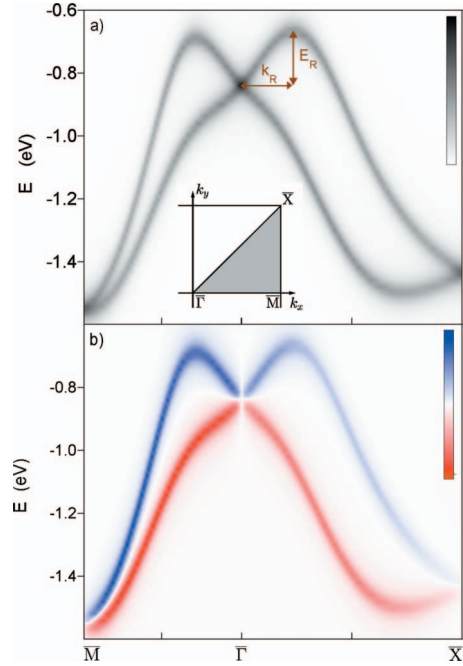


FIG. 3. (Color) Surface states in Bi/BaTiO<sub>3</sub>(001) for  $P_{\uparrow}$ . (a) Spin-integrated Bloch spectral density for Bi imaged as gray scale (white 0, black 400 states/Hartree) along  $\bar{M}-\bar{\Gamma}-\bar{X}$  of the two-dimensional Brillouin zone. The Rashba splitting  $k_R$  and the Rashba energy  $E_R$  are indicated. The inset shows a quarter of the Brillouin zone. (b) Spin-resolved density for Bi depicted as color scale. Blue (red) indicates a positive (negative) difference  $n^{\uparrow}-n^{\downarrow}$ , with the spin projection normal to  $\mathbf{k}_{\parallel}$  and with extrema of  $\pm 150$  states/Hartree. Energy scale as in Fig. 2.

toward  $-z$ , referred to as  $P_{\downarrow}$ , the  $z$  coordinates of Ti and O sites in the same layer obey  $z_{\text{Ti}} < z_{\text{O}}$  ( $z_{\text{Ti}} - z_{\text{O}} = -0.09 \text{ \AA}$ ). The opposite case is referred to as  $P_{\uparrow}$ , with  $z_{\text{Ti}} > z_{\text{O}}$ .

A total-energy analysis shows that Bi forms a  $1 \times 1$  adlayer, with Bi on top of the Ba atoms of the subsurface BaO layer (Fig. 1 for  $P_{\uparrow}$ ; all results for  $P_{\downarrow}$  agree qualitatively with those for  $P_{\uparrow}$  and are therefore not shown). Their distance in  $z$  direction to the surface Ti sites is  $2.11 \text{ \AA}$  for  $P_{\uparrow}$ , which is

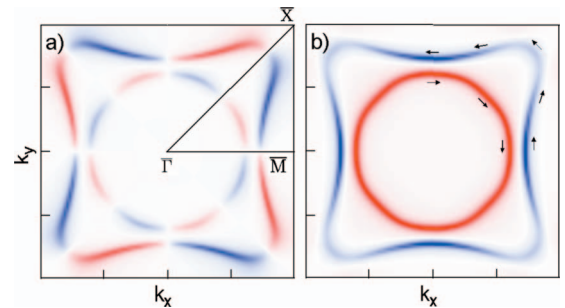


FIG. 4. (Color) Spin topology of the surface states in Bi/BaTiO<sub>3</sub>(001) for  $P_{\uparrow}$ . (a) Radial and (b) tangential spin polarization components are visualized as the difference  $n^{\uparrow}-n^{\downarrow}$  of Bloch spectral densities at Bi in the entire two-dimensional Brillouin zone. The energy is  $-1.30 \text{ eV}$  (energy scale as in Fig. 2). Dark blue and red indicate  $+150$  and  $-150$  states/Hartree, respectively. Arrows in (b) give a visual impression of the total spin polarization.

TABLE I. Rashba effect in Bi/BaTiO<sub>3</sub>. The splitting  $k_R$ , the Rashba energy  $E_R$ , the effective mass  $m^*$  (in units of the electron mass  $m_e$ ), and the Rashba parameter  $\gamma_R$  for both bulk electric polarization  $P_\uparrow$  and  $P_\downarrow$  are given for the  $\bar{\Gamma}-\bar{M}$  and the  $\bar{\Gamma}-\bar{X}$  direction of the two-dimensional Brillouin zone [inset in Fig. 3(a)].

|                | $\bar{\Gamma}-\bar{M}$         |               |                    |                                  | $\bar{\Gamma}-\bar{X}$         |               |                    |                                  |
|----------------|--------------------------------|---------------|--------------------|----------------------------------|--------------------------------|---------------|--------------------|----------------------------------|
|                | $k_R$<br>( $\text{\AA}^{-1}$ ) | $E_R$<br>(eV) | $m^*$<br>( $m_e$ ) | $\gamma_R$<br>(eV $\text{\AA}$ ) | $k_R$<br>( $\text{\AA}^{-1}$ ) | $E_R$<br>(eV) | $m^*$<br>( $m_e$ ) | $\gamma_R$<br>(eV $\text{\AA}$ ) |
| $P_\uparrow$   | 0.22                           | 0.16          | -1.14              | 1.45                             | 0.25                           | 0.18          | -1.36              | 1.42                             |
| $P_\downarrow$ | 0.23                           | 0.16          | -1.22              | 1.39                             | 0.27                           | 0.18          | -1.48              | 1.36                             |

equivalent to 52.9% of the bulk Ba-Ba  $z$  distance (3.99  $\text{\AA}$ ). For  $P_\downarrow$  we find a  $z$  distance of 2.16  $\text{\AA}$  (54.0%).

It turns out that for both  $P_\uparrow$  and  $P_\downarrow$ , the polarization at the topmost TiO<sub>2</sub> layer is negative (i. e.,  $z_{\text{Ti}} < z_{\text{O}}$ ).<sup>28</sup> However, the relaxations of these atoms differ:  $z_{\text{Ti}} - z_{\text{O}} = -0.13$   $\text{\AA}$  for  $P_\uparrow$  and  $-0.18$   $\text{\AA}$  for  $P_\downarrow$ . In summary, the surface geometry depends slightly on the orientation of the bulk electric polarization.

#### IV. RASHBA SPLITTING IN THE Bi SURFACE STATES

The Bi adlayer gives rise to occupied  $6p$  electronic states in the fundamental band gap of the surface BaTiO<sub>3</sub> stack. At  $\bar{\Gamma}$  these show up at energies  $E_0 = -0.82$  eV for  $P_\uparrow$  (arrow in Fig. 2) and at  $-0.84$  eV for  $P_\downarrow$ , respectively. These are mostly confined to the Bi layer but show also considerable spectral weight in the adjacent layer, making them subject to switching of  $\mathbf{P}$ .

The dispersions of the Bi surface states show the typical signatures of the Rashba splitting:  $k_R$  and the Rashba energy  $E_R$  which are indicated in Fig. 3(a). Since the dispersion is anisotropic, the characteristics of the Rashba splitting are anisotropic as well (Table I). Although the origin of this anisotropy are higher-order terms in  $\mathbf{k}_\parallel$ ,<sup>29</sup> we quantify the effect by means of an anisotropic effective mass and Rashba parameter.

The switching of the electric polarization  $\mathbf{P}$  affects indeed the Rashba splitting  $k_R$  (Table I), thereby confirming the above motivation. The strength of this spin-electric coupling is quantified by the relative change in  $k_R$ ; for  $\bar{\Gamma}-\bar{M}$  it is about 4.5% whereas for  $\bar{\Gamma}-\bar{X}$  it is about 5.5%. These numbers are qualitatively explained on one hand by the weak polarization dependence of the surface geometry and on the other hand by the strong localization of the Bi  $6p$  states to the adlayer. Both a larger relaxation and a stronger hybridization of the Bi states with those of the substrate could enhance the effect. We would like to stress that the relative change in the surface magnetization of a single Fe layer on BaTiO<sub>3</sub>(001) is 2.8%;<sup>20</sup> this shows that the spin-electric coupling is at least as large as the magnetoelectric coupling.

The average splitting  $k_R$  of about 0.24  $\text{\AA}^{-1}$  is sizably larger than the unmatched 0.13  $\text{\AA}^{-1}$  reported for Bi/Ag(111).<sup>13</sup> However,  $E_R$  is with about 0.170 eV less than in Bi/Ag(111) (0.200 eV). Consequently, the effective masses  $m^* = -\hbar^2 k_R^2 / (2E_R)$  of Bi/BaTiO<sub>3</sub> are larger (in absolute value) than in Bi/Ag(111) ( $-0.32m_e$ ). Because the

Rashba parameter of the free-electron model depends on  $m^*$ , the numerical values for  $\gamma_R = 2|E_R|/k_R$  in Bi/BaTiO<sub>3</sub> are considerable less than that in Bi/Ag(111) (3.08 eV  $\text{\AA}$ ), although the splitting in reciprocal space is about as twice as large.

We note that relevant for applications is not the strength  $\gamma_R$  of the Rashba spin-orbit coupling but the actual splitting  $k_R$ . A large splitting in reciprocal space is equivalent to a small wavelength in direct space. As a consequence, the spatial range in which the electronic wave functions of the split states can effectively interfere in a spin electronics device is small as well. This feature is favorable since it allows reduced device dimensions.

#### V. MOMENTUM DISTRIBUTIONS AND SPIN TOPOLOGY OF THE Bi SURFACE STATES

Momentum distributions which display the Bloch spectral density versus  $k_\parallel$  at fixed energy  $E$  (Fig. 4) deviate significantly from the circular momentum distributions of the free-electron model, in accordance with the dispersion relations (Fig. 3). The anisotropy shows up in particular for the outer band (with larger  $|k_\parallel|$ ) which reflects the  $4mm$  symmetry of the surface.

Another signature of the Rashba effect—besides  $k_R$  and  $E_R$ —is the spin polarization  $\mathbf{S}_\pm$  of the split electronic states. For free electrons,  $\mathbf{S}_\pm$  lies within the confinement plane, is tangential to the circular momentum distribution and is complete ( $|\mathbf{S}_\pm| = 100\%$ ). For Bi/BaTiO<sub>3</sub> we find in-plane  $\mathbf{S}_\pm$  but also distinct deviations from the free-electron model, as is exemplified at  $E = -1.30$  eV (Fig. 4). The inner state, with small  $|k_\parallel|$ , compares well with the free-electron model; confer the almost circular momentum distribution with small radial component (a) and constant tangential component (b). The outer state, with larger  $|k_\parallel|$ , shows a large tangential component, in particular along  $\bar{\Gamma}-\bar{M}$ , but significantly less along  $\bar{\Gamma}-\bar{X}$ . This together with the shape of its sizable radial component implies that its spin follows the curvature of its noncircular momentum distribution [arrows in Fig. 4(b)].

#### VI. CONCLUDING REMARKS

Our theoretical investigation provides a proof of concept for spin-electric coupling in an adlayer of a heavy  $p$  metal on

a ferroelectric substrate: Switching of the intrinsic electric polarization  $\mathbf{P}$  in the ferroelectric (here: BaTiO<sub>3</sub>) affects the strength of the Rashba splitting in the adlayer (here: Bi).

The present work predicts a moderate spin-electric coupling but a large absolute Rashba-type spin splitting. Nevertheless, it is conceivable to increase the effect by larger atomic displacements in particular at the ferroelectric/adlayer interface. A possible candidate might be PbTiO<sub>3</sub> which shows larger displacements and electric polarizations than BaTiO<sub>3</sub>.<sup>28</sup>

We encourage to search for improved Rashba-split/ferroelectric systems in both theory and experiment. The ultimate spin-electric coupling would be a change in sign of the Rashba parameter  $\gamma_R$ —and hence of the spin polarization  $\mathbf{S}$ —upon reversal of  $\mathbf{P}$ .

We appreciate very much fruitful discussions with M. Fechner and Chr. R. Ast. This work is supported by the *Sonderforschungsbereich* 762 “Functionality of Oxide Interfaces.”

\*Corresponding author; henk@mpi-halle.de

- <sup>1</sup>I. Žutić, J. Fabian, and S. Das Sarma, *Rev. Mod. Phys.* **76**, 323 (2004).
- <sup>2</sup>W. Eerenstein, N. D. Mathur, and J. F. Scott, *Nature (London)* **442**, 759 (2006).
- <sup>3</sup>S.-W. Cheong and M. Mostovoy, *Nature Mater.* **6**, 13 (2007).
- <sup>4</sup>H. Béa, M. Gajek, M. Bibes, and A. Barthélémy, *J. Phys.: Condens. Matter* **20**, 434221 (2008).
- <sup>5</sup>Y. A. Bychkov and E. I. Rashba, *J. Phys. C* **17**, 6039 (1984).
- <sup>6</sup>S. Datta and B. Das, *Appl. Phys. Lett.* **56**, 665 (1990).
- <sup>7</sup>N. Samarth, in *Solid State Physics* Vol. 58, edited by H. Ehrenreich and F. Spaepen (Elsevier, Amsterdam, 2004), p. 1.
- <sup>8</sup>H. C. Koo, J. H. Kwon, J. Eom, J. Chang, S. H. Han, and M. Johnson, *Science* **325**, 1515 (2009).
- <sup>9</sup>R. Winkler, *Spin-Orbit Coupling Effects in Two-Dimensional Electron and Hole Systems* (Springer, Berlin, 2003).
- <sup>10</sup>L. Petersen and P. Hedegård, *Surf. Sci.* **459**, 49 (2000).
- <sup>11</sup>F. Reinert, *J. Phys. Condens. Matter* **15**, S693 (2003).
- <sup>12</sup>J. H. Dil, *J. Phys. Condens. Matter* **21**, 403001 (2009).
- <sup>13</sup>C. R. Ast, J. Henk, A. Ernst, L. Moreschini, M. C. Falub, D. Pacilé, P. Bruno, K. Kern, and M. Grioni, *Phys. Rev. Lett.* **98**, 186807 (2007).
- <sup>14</sup>I. Gierz, T. Suzuki, E. Frantzeskakis, S. Pons, S. Ostanin, A. Ernst, J. Henk, M. Grioni, K. Kern, and C. R. Ast, *Phys. Rev. Lett.* **103**, 046803 (2009).
- <sup>15</sup>C. R. Ast, D. Pacilé, L. Moreschini, M. C. Falub, M. Papagno, K. Kern, M. Grioni, J. Henk, A. Ernst, S. Ostanin, and P. Bruno, *Phys. Rev. B* **77**, 081407(R) (2008).
- <sup>16</sup>L. Moreschini, A. Bendounan, C. R. Ast, F. Reinert, M. Falub, and M. Grioni, *Phys. Rev. B* **77**, 115407 (2008).
- <sup>17</sup>H. Bentmann, F. Forster, G. Bihlmayer, E. V. Chulkov, L. Moreschini, M. Grioni, and F. Reinert, *Europhys. Lett.* **87**, 37003 (2009).
- <sup>18</sup>C.-G. Duan, S. S. Jaswal, and E. Y. Tsymlal, *Phys. Rev. Lett.* **97**, 047201 (2006).
- <sup>19</sup>J. P. Velev, C.-G. Duan, K. D. Belashchenko, S. S. Jaswal, and E. Y. Tsymlal, *J. Appl. Phys.* **103**, 07A701 (2008).
- <sup>20</sup>M. Fechner, I. V. Maznichenko, S. Ostanin, A. Ernst, J. Henk, P. Bruno, and I. Mertig, *Phys. Rev. B* **78**, 212406 (2008).
- <sup>21</sup>C. Jia and J. Berakdar, *Appl. Phys. Lett.* **95**, 012105 (2009).
- <sup>22</sup>O. Krupin, G. Bihlmayer, K. Starke, S. Gorovikov, J. E. Prieto, K. Döbrich, S. Blügel, and G. Kaindl, *Phys. Rev. B* **71**, 201403(R) (2005).
- <sup>23</sup>S. Prakash, M. B. Karacor, and S. Banerjee, *Surf. Sci. Rep.* **64**, 233 (2009).
- <sup>24</sup>H. Mirhosseini, J. Henk, A. Ernst, S. Ostanin, C.-T. Chiang, P. Yu, A. Winkelmann, and J. Kirschner, *Phys. Rev. B* **79**, 245428 (2009).
- <sup>25</sup>G. Kresse and D. Joubert, *Phys. Rev. B* **59**, 1758 (1999).
- <sup>26</sup>*Electron Scattering in Solid Matter*, edited by J. Zabloudil, R. Hammerling, L. Szunyogh, and P. Weinberger (Springer, Berlin, 2005).
- <sup>27</sup>Forschungszentrum Jülich, Institut für Festkörperforschung, Institute Quantum Theory of Materials, D-52425 Jülich, Germany.
- <sup>28</sup>M. Fechner, S. Ostanin, and I. Mertig, *Phys. Rev. B* **77**, 094112 (2008).
- <sup>29</sup>T. Oguchi and T. Shishidou, *J. Phys.: Condens. Matter* **21**, 092001 (2009).